JOC The Journal of Organic Chemistry

Article

pubs.acs.org/joc

Quantitative DNA Interstrand Cross-Link Formation by Coumarin and Thymine: Structure Determination, Sequence Effect, and Fluorescence Detection

Huabing Sun, Heli Fan, and Xiaohua Peng*

Department of Chemistry and Biochemistry, University of Wisconsin-Milwaukee, 3210 North Cramer Street, Milwaukee, Wisconsin 53211, United States

Supporting Information

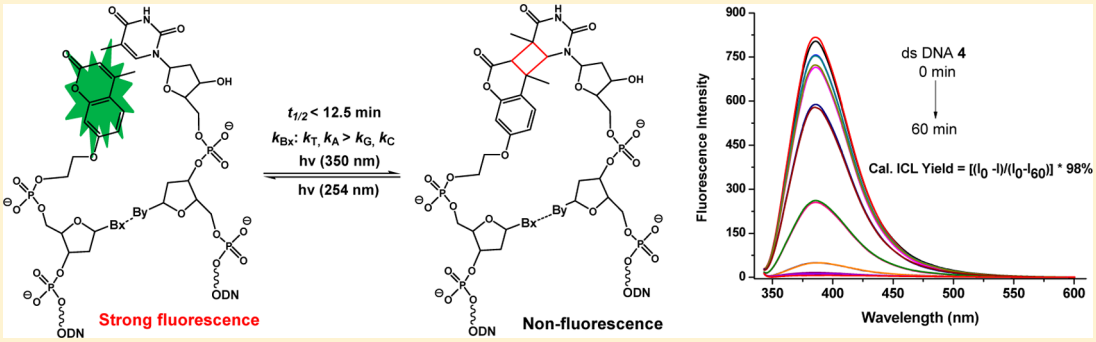

ABSTRACT: The coumarin analogues have been widely utilized in medicine, biology, biochemistry, and material sciences. Here, we report a detailed study on the reactivity of coumarins toward DNA. A series of coumarin analogues were synthesized and incorporated into oligodeoxynucleotides. A photoinduced [2 + 2] cycloaddition occurs between the coumarin moiety and the thymidine upon 350 nm irradiation forming both *syn*- and *anti*-cyclobutane adducts (**17** and **18**), which are photoreversible by 254/350 nm irradiation in DNA. Quantitative DNA interstrand cross-link (ICL) formation was observed with the coumarin moieties containing a flexible two-carbon or longer chain. DNA cross-linking by coumarins shows a kinetic preference when flanked by an A:T base pair as opposed to a G:C pair. An efficient photoinduced electron transfer between coumarin and dG slows down ICL formation. ICL formation quenches the fluorescence of coumarin, which, for the first time, enables fast, easy, and real-time monitoring of DNA cross-linking and photoreversibility via fluorescence spectroscopy. It can be used to detect the transversion mutation between pyrimidines and purines. Overall, this work provides new insights into the biochemical properties and possible toxicity of coumarins. A quantitative, fluorescence-detectable, and photoswitchable DNA cross-linking reaction of the coumarin moieties can potentially serve as mechanistic probes and tools for bioresearch without disrupting native biological environment.

INTRODUCTION

DNA interstrand cross-links (ICLs) inhibit DNA replication and gene expression by preventing strand separation. Cross-linking agents have been widely applied in cancer therapy,[1] study of DNA repair and gene regulation,[2−6] protein−DNA binding,[7−9] and DNA nanotechnology.[10] Most DNA cross-linking processes are irreversible. Reversible reactions provide opportunities for the development of new applications.[11−16] For example, the reversible alkylation reactions induced by anticancer drug ecteinascidin 743 allow migration of the alkylating sites to achieve sequence selectivity and anticancer activity.[11] The reversibility of DNA-drug adducts was also correlated with the cytotoxicity of antitumor drugs based on cyclopropylpyrroloindole.[12] Most recently, Rokita and co-workers discovered the reversible nature of quinone methide which offers a novel strategy for cell-compatible target selective alkylation that allows for strand exchange and cross-link migration leading to dynamic cross-linking.[13−16]

Many photoactive molecules allowing reversible photochemical reactions are widely used in polymer sciences, such as light switchable coatings and drug delivery.[17,18] Photoactive molecules have also been studied for reversible photo-cross-linking and photomanipulation of DNA.[19−25] For instance, psoralens, a class of naturally occurring photoreactive products, form interstrand cross-links (ICLs) in duplex and triplex DNA, which have been utilized for DNA damage and repair study, for therapeutic gene modulation, and as photoactive probes of nucleic acid structure and function.[20−23,26,27] Coumarin molecules, with similar structure scaffold as psoralens, are capable of photoreversible dimerization via a photoinduced [2 + 2] cycloaddition reaction and subsequent photocleavage at a different wavelength.[28] They have wide polymeric applications, such as electroluminescence studies, light and energy harvest-

Received: July 2, 2014

   dx.doi.org/10.1021/jo5014756 | J. Org. Chem. XXXX, XXX, XXX−XXX

Scheme 1. Synthesis of the Phosphoramidites 8−13

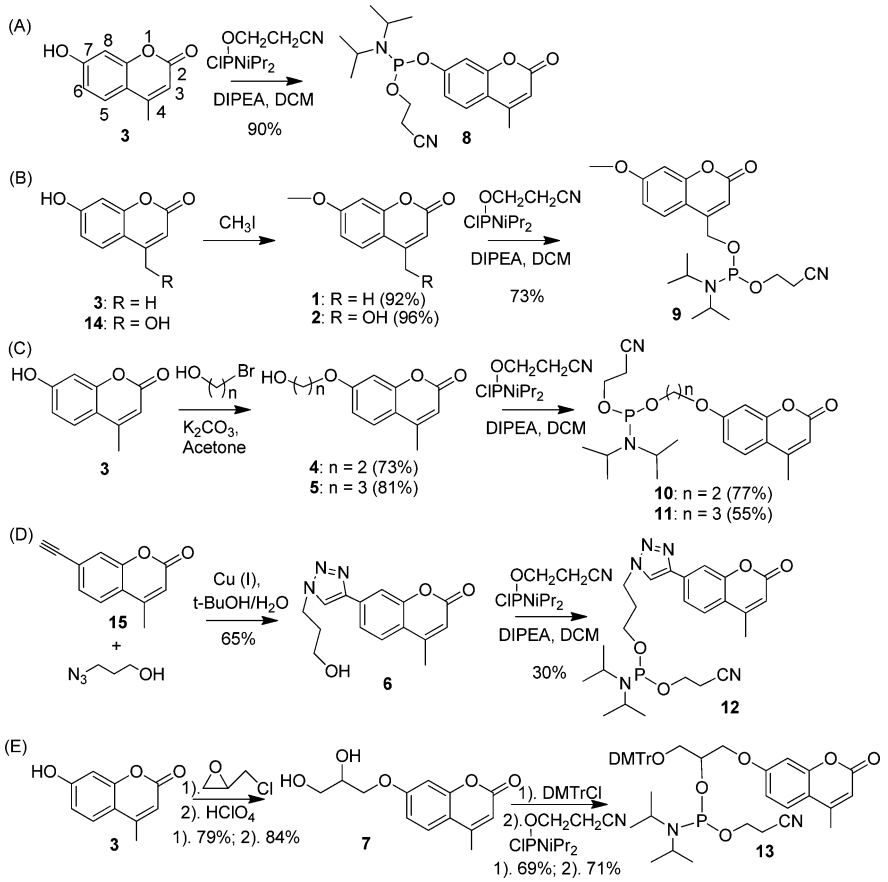

ing, construction of liquid crystalline polymers and photoactive surfaces, and photoreversible polymerization, chain extension, and cleavage.[28] In addition to polymer science, coumarin analogues are also used in the field of biological science as medicines or as fluorescent tags and fluoroprobes for labeling protein and nucleic acids.[28,29] However, to the best of our knowledge, there is no detailed information on the photoreactivity of coumarin with biomolecules such as DNA, RNA, and proteins.

Recently, we have shown that a coumarin-modified thymidine is capable of cross-linking dT upon 350 nm irradiation with about 69% cross-linking yield.[30] Such a process is photoswitchable and leads to fluorescence variation. However, the cross-linking efficiency by a coumarin-modified thymidine is too low to allow online fluorescence detection of DNA cross-linking. In addition, coumarins with suitable linkers can be directly incorporated into DNA at any position instead of attaching to thymidine in our previous study, which could avoid the intramolecular reaction between coumarin and thymidine. We envisage that the photochemistry of coumarin or coumarin-containing ODN would enable a method for real-time monitoring of the cross-linking process via fluorescence spectroscopy if quantitative DNA cross-linking can be achieved, which is indispensable for direct measurement of the cross-link formation and expanding its bioapplication. These predictions have been experimentally borne out by detailed investigations on the photoactivity of coumarin-derived compounds toward DNA. However, the chemistry is more complex than we expect. Here, we report the structure of coumarin-dT dimers and a quantitative, fluorescence-detectable, sequence-dependent, and photoswitchable DNA ICL formation via coumarin moieties. Most traditional methods for DNA ICL analysis require radiolabeling with ^{32}P, ^{14}C, or ^{3}H which are considered to be health and safety hazards. In addition, they are offline methods and are time-consuming. Our methodology is capable of a safe real-time detection of ICL formation, which will undoubtedly facilitate its bioapplication.

RESULTS AND DISCUSSION

Design and Synthesis of the Cross-Linking Precursor and Their Incorporation into Oligodeoxynucleotides. We designed and synthesized seven coumarin analogues **1**−**7** with various modifications at position 4 (**2**) or 7 (**3**−**7**), which allowed us to study the reaction sites and linker effects on the cross-linking efficiency (Scheme 1). Compounds **2**−**7** contain a hydroxyl group which can be converted to the corresponding phosphoramidites **8**−**13** used for solid-phase DNA synthesis. Compounds **2** and **3** were designed to study the effect of the phosphorus position on the cross-linking efficiency, while **3**−**6** were used to investigate the effect of the linker length and **7** allows for flexible incorporation into DNA at any positions. Compound **1** or **2** was prepared via methylation of 7-hydroxy-2*H*-chromen-2-one derivative **3** or **14**, respectively (Scheme 1B). Three different linker units were introduced to compound **3** via Williamson ether synthesis yielding **4**, **5**, and **7** (Scheme 1C and E). Compound **6** was synthesized by "click" reaction between 3-azidopropan-1-ol and 7-ethynyl-4-methyl-2*H*-chromen-2-one (**15**) (Scheme 1D). All coumarin monomers with the hydroxyl group (**2**−**7**) were converted to the corresponding phosphoramidites (**8**−**13**) using standard methods (Scheme

dx.doi.org/10.1021/jo5014756 | J. Org. Chem. XXXX, XXX, XXX−XXX

Scheme 2. Double-Stranded DNAs Used in This Study and Their Melting Temperatures

ds DNA-**1** (T_M: 57.8 ± 0.1°C)
ODN **1a**: 3'-dTATACGGCGGGT
ODN **1b**: 5'-dATATGCCGCCCA

ds DNA-**2** (T_M: 59.8 ± 0.1°C)
ODN **1a**: 3'-dTATACGGCGGGT
ODN **2b**: 5'-d**2**TATGCCGCCCA

ds DNA-**3** (T_M: 58.9 ± 0.7°C)
ODN **1a**: 3'-dTATACGGCGGGT
ODN **3b**: 5'-d**3**TATGCCGCCCA

ds DNA-**4** (T_M: 60.7 ± 1.0°C)
ODN **1a**: 3'-dTATACGGCGGGT
ODN **4b**: 5'-d**4**TATGCCGCCCA

ds DNA-**5** (T_M: 60.9 ± 0.8°C)
ODN **1a**: 3'-dTATACGGCGGGT
ODN **5b**: 5'-d**5**TATGCCGCCCA

ds DNA-**6** (T_M: 59.2 ± 1.2°C)
ODN **1a**: 3'-dTATACGGCGGGT
ODN **6b**: 5'-d**6**TATGCCGCCCA

ds DNA-**7**
ODN **7a**: 3'-dTTTACGGCGGGT
ODN **7b**: 5'-d**4**AATGCCGCCCA

ds DNA-**8**
ODN **8a**: 3'-dTCTACGGCGGGT
ODN **8b**: 5'-d**4**GATGCCGCCCA

ds DNA-**9**
ODN **9a**: 3'-dTGTACGGCGGGT
ODN **9b**: 5'-d**4**CATGCCGCCCA

ds DNA-**10**
ODN **10a**: 3'-dGCGTTTTTAGCC
ODN **10b**: 5'-dCGCAA**7**AATCGG

ds DNA-**11a-c**
ODN **11a-c**: 3'-d**X**AAGTACGGCGGGTACG
ODN **11**: 5'-d**4**TTCATGCCGCC

a: X = T;
b: X = A;
c: X = G

ds DNA-**12**
ODN **12a**: 3'-dTTTTTACGGCGGGTACCCGGATTCCAAGTACGGCTAGTACGTCCTTGACA
ODN **7b**: 5'-d**4**AATGCCGCCCA

ds DNA-**13**
ODN **12a**: 3'-dTTTTTACGGCGGGTACCCGGATTCCAAGTACGGCTAGTACGTCCTTGACA
ODN **13b**: 5'-dAA**7**AATGCCGCCCA

1A–E). All new compounds and phosphoramidites were confirmed by NMR and HRMS (Supporting Information (SI), Figures S23a–30d).

ODNs containing **2**–**7** were prepared using commercially available β-cyanoethyl phosphoramidites containing phenoxyacetyl protecting groups on the exocyclic amines of dA and dG, which allowed a very mild deprotection condition avoiding the decomposition of the functionalized ODNs (**2b**–**10b**, **11**, and **13b**) (Scheme 2). All ODNs were purified by 20% denaturing polyacrylamide gel electrophoresis (PAGE) and characterized by MALDI-TOF-MS (SI, Table S2 and Figures S35–45).

After successfully synthesizing the ODNs containing coumarin moieties, we studied the effect of coumarin on duplex thermal stability by measuring the UV-melting temperatures (T_M) (Scheme 2). The coumarin moieties increased the T_M (1.1–3.1 °C) relative to when 2′-deoxyadenosine (dA) was present, possibly due to the increased π–π stacking and/or increased lipophilicity.[31−33] The T_M increase was more obvious when coumarin was incorporated into ODNs via position 4 (ds DNA-**2**, ΔT_M = 2.0 °C) than via position 7 (ds DNA-**3**, ΔT_M = 1.1 °C). A flexible linker unit at position 7 further enhances the duplex stability by about 3.0 °C (ds DNA-**4**, ΔT_M = 2.9 °C; ds DNA-**5**, ΔT_M = 3.1 °C). A triazole moiety with less flexibility in stacking and decreased lipophilicity seems less favorable for duplex stability (ds DNA-**6**) than an alkyl chain (ds DNA-**5**).

Monomer Reaction. Previously, we have utilized LC-MS to analyze the cross-linked adduct formed between coumarin and dT, while the detailed structure was not elucidated due to the difficulty isolating the adducts in amounts sufficient for NMR analysis.[30] Here, we studied the reactivity of coumarin moiety with canonical nucleosides dA, dG, dT, and dC using compound **1** as a representative. Initially, LC-MS was used to monitor the reaction. A new product with a mass of 455.4 (corresponding to *syn*- and *anti*-cyclobutane **1**-dT dimers **17** and **18**) was detected in the presence of dT after 350 nm irradiation for 2 days, while no new products were formed between **1** and dC, dA, or dG (SI, Figure S31a–d). In addition to **17** and **18**, a coumarin dimer **19** was also isolated. All compounds were characterized by ^{1}H NMR, ^{13}C NMR, and HRMS (SI, Figures S32a–34c). They were formed by a [2 + 2] cycloaddition reaction. Two isomers **17** and **18** were formed between **1** and dT, while syn-adduct **17** was the predominant product (yield: 15% for **17** and 9% for **18**) (Scheme 3). The final structure of **17** and **18** was determined by two-dimensional nuclear magnetic resonance spectroscopy (H–H COSY). Formation of **17**–**19** quenches the fluorescence of coumarin due to the disruption of conjugated π-system (Figure 1).

Effect of Linker Position and Length on DNA Cross-Linking. The monomer reactions indicated that the coumarin moiety can react with dT. To study its reactivity in DNA, we designed six double stranded (ds) DNAs (**1**–**6**) and investigated the DNA interstrand cross-linking efficiency (Scheme 2). The ds DNA-**2**–**6** contain a coumarin moiety opposing dT, while ds DNA-**1** has an A:T base pair which is used as a control. All DNA duplexes were photoirradiated at 350 nm. A wavelength of 350 nm was chosen because near-UV light (>300 nm) is compatible with living cells and is almost not absorbed by most biological molecules other than the

dx.doi.org/10.1021/jo5014756 | J. Org. Chem. XXXX, XXX, XXX–XXX

Scheme 3. Photo-Induced [2 + 2] Cycloaddition between 1 and dT

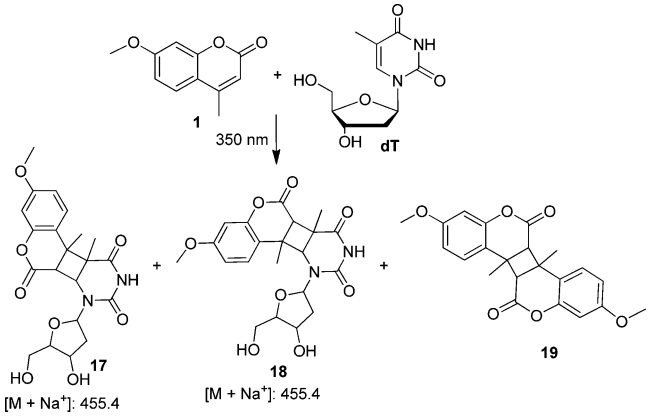

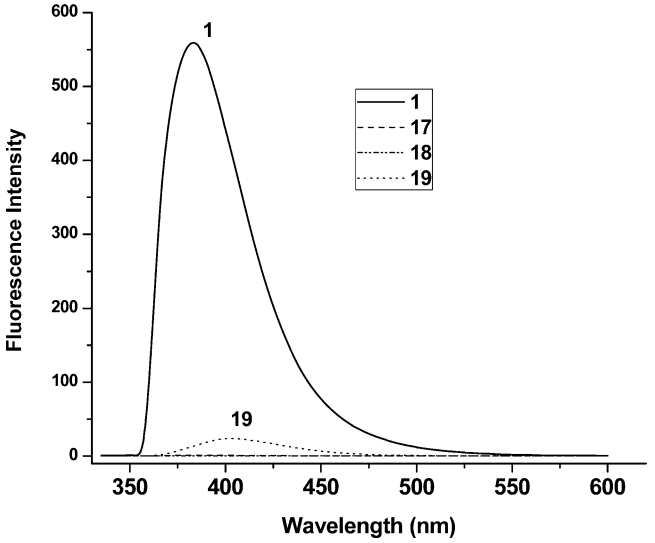

Figure 1. Fluorescence emission spectra of coumarin **1** and dimers **17**–**19** (10 μM, λ_{ex} = 325 nm, slit width = 15 nm; λ_{em} = 385 nm, slit width = 2.5 nm).

coumarin-modified ODNs. Irradiation of ds DNA-**2**–**6** resulted in a new band which migrates more slowly than unreacted ODN, indicative of the formation of interstrand cross-linked material (SI, Figures S46–49), while this was not observed with native ds DNA-**1** (Figure 2). A higher ICL yield was observed with ds DNA-**3** (86%, lane 3) compared to ds DNA-**2** (3%, lane 2). As cycloaddition reaction occurs at positions 3 and 4, coumarin moiety **2** attached to ODN via position-4 may induce

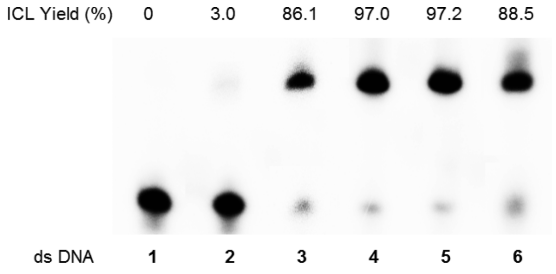

Figure 2. Phosphorimage autoradiogram of denaturing PAGE analysis of ICL formation (100 nM ds DNA-**1**–**6** was irradiated at 350 nm for 2 h; ODN **1a** was 5′-[^{32}P]-labeled).

steric hindrance for the ICL formation, while compounds **3**–**6** may adopt a more favorable conformation for producing a highly efficient transition state between coumarin moieties and dT.

The coumarin reactivity in DNA can be further tuned by altering the linker units between the phosphate group and the coumarin moiety. For example, compound **3** without a linker led to a relatively low ICL yield (86%, lane 3) because of the lack of flexibility, while quantitative ICL yields were observed with ds DNA-**4** and **5** with an adaptable chain between the phosphate group and coumarin moiety (Figure 2, lanes 4 and 5). The rate constants for ds DNA-**4** and **5** were 5–6 times the rate constant for ds DNA-**3** (Table 1 and SI, Figure S2–3).

Table 1. ICL Formation Reaction Rates for DNA Duplexes with Different Coumarin Moieties

entry	k (10^{-4} s^{-1})	$t_{1/2}$ (min)
ds DNA-**2**	*n.d.*[a]	*n.d.*
ds DNA-**3**	9.5 ± 1.6	12.4 ± 2.0
ds DNA-**4**	50.4 ± 3.8	2.3 ± 0.2
ds DNA-**5**	53.9 ± 4.1	2.3 ± 0.2
ds DNA-**6**	9.8 ± 1.1	11.9 ± 1.2

[a]*n.d.*: not determined.

However, installation of a triazole ring in **6** decreases the reactivity possibly due to an electron transfer in the excitation state of coumarin. In summary, compounds **4** and **5** enable highly efficient and fast DNA interstrand cross-linking with quantitative ICL yields and a 2.3 min half-life (Table 1 and SI, Figure S1a,b). Finally, compound **4** was chosen for further study.

Flanking Sequence Effect on DNA Cross-Linking and the Fluorescence Intensity of the Coumarin Moiety. In addition to the linker units, flanking bases also have a great effect on cross-linking. Although **4** efficiently forms DNA ICLs when flanked by all four bases, lower ICL yields were observed when **4** was flanked by dC (ds DNA-**9**: 88% vs quantitative ICL formation for ds DNA-**4**: 98%, **7**: 100%, or **8**: 97%) (Figure 3).

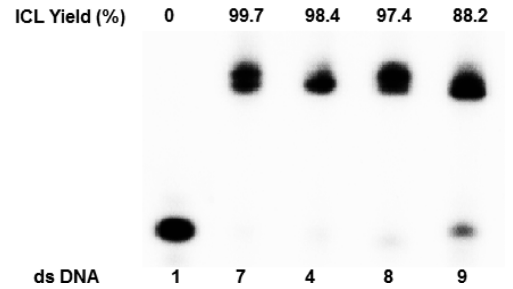

Figure 3. Phosphorimage autoradiogram of denaturing PAGE analysis of ICL formation (100 nM ds DNAs-**1**, **4**, and **7**–**9** were irradiated at 350 nm for 2 h; ODNs without coumarin were 5′-[^{32}P]-labeled).

Moreover, the rate constant for cross-link formation in ds DNA-**8** or **9**, where **4**/dT was flanked by a G:C base pair, was ~10 times slower than when **4**/dT was flanked by a T:A pair (ds DNA-**4** and **7**) (Table 2 and SI, Figures S2b, S3b, S4, and S5). ICL formation with ds DNA-**7** and ds DNA-**4** upon 350 nm irradiation was complete within 10 min with more than 95% cross-linking yield, while it took more than 120 min with ds DNA-**8** and **9** (SI, Figure S1b).

dx.doi.org/10.1021/jo5014756 | J. Org. Chem. XXXX, XXX, XXX–XXX

Table 2. Rate of ICL Formation or Cleavage of DNAs Containing 4 with Different Flanking Bases

(ds DNA-4 and 7–9: 3′-dTYTACGGCGGGT ● 5′-d4XATGCCGCCCA)							
		k (ICL Formation, 10^{-4} s^{-1})		$t_{1/2}$ (min)			
entry	X:Y	*p.d.*[a]	*f.d.*	*p.d.*	*f.d.*	k_c (Cleavage, 10^{-3} s^{-1})	$t_{1/2}$ (min)
ds DNA-**7**	A:T	42.0 ± 4.0	31.7 ± 0.4	2.7 ± 0.2	3.6 ± 0.1	4.6 ± 0.2	2.5 ± 0.1
ds DNA-**4**	T:A	50.4 ± 3.8	46.6 ± 2.7	2.3 ± 0.2	2.5 ± 0.2	4.0 ± 0.5	2.9 ± 0.4
ds DNA-**8**	G:C	5.8 ± 0.2	6.8 ± 0.2	20.0 ± 0.8	16.9 ± 0.6	17.1 ± 0.1	0.7 ± 0.0
ds DNA-**9**	C:G	4.1 ± 0.1	5.1 ± 1.2	28.1 ± 1.0	22.8 ± 5.5	12.2 ± 1.2	1.0 ± 0.2

[a]*p.d.*: determined by radioactive ^{32}P-labeling method; *f.d.*: determined by fluorescence assay.

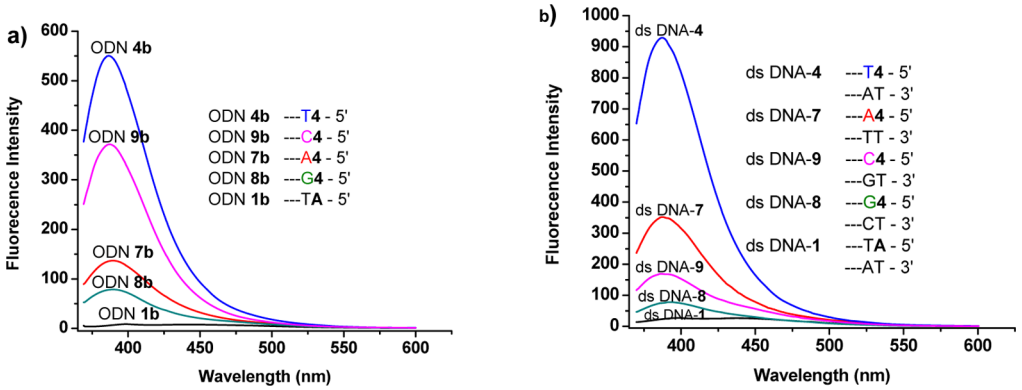

Figure 4. Comparison of fluorescence intensity of **4** when flanked by different nucleotides: (a) fluorescence emission spectra of 10 μM single-stranded ODNs; (b) fluorescence emission spectra of 10 μM duplexes (measured in 100 mM NaCl and 10 mM pH 7 phosphate buffer solution with λ_{ex} = 350 nm, slit width = 10 nm; λ_{em} = 390 nm, slit width = 10 nm).

We also observed that the flanking sequences greatly affect the fluorescence intensity of the coumarin moiety. The ODNs (**7b** and **8b**) with the coumarin moiety adjacent to a purine nucleoside showed a greatly decreased fluorescence intensity in comparison with those (**4b** and **9b**) containing **4** flanking to a pyrimidine nucleoside (Figure 4a). It is well-known that the photoinduced electron transfer leads to nucleobase-specific fluorescence quenching.[34] We propose that the excited coumarin **4** is able to oxidize other nucleobases due to its large excited state reduction potentials (2.10 V determined by cyclic voltammetry, SI, Figure S6). The sequence of the fluorescence quenching efficiency is on the order of dG > dA > dC ≈ dT, which is equivalent to the order of nucleobase oxidation potentials ($E_{O,CV}$: G (1.25), A (1.72), C (1.87), and T (1.90)).[35] This observation is consistent with Seidel's report.[34] Interestingly, hybridization of DNAs further enhances the fluorescence of ds DNA-**4** and **7** with an A:T base pair next to **4**:T, and quenches the fluorescence of ds DNA-**9** and **8** with a G:C pair adjacent to **4**:T (Figure 4b). Overall, the sequence of the fluorescence quenching efficiency is consistent with the order of the DNA cross-linking rate constant $k_{ds\text{-}4}$, $k_{ds\text{-}7} \gg k_{ds\text{-}8}$, $k_{ds\text{-}9}$. The correlation between the quenching efficiency and the ICL formation constant indicates that the photoinduced electron transfer plays an important role in decreased ICL formation when **4** is adjacent to a G:C pair.

Fluorescence Detection of DNA Cross-Linking Formation. Similar to the monomer study, no fluorescence was observed with the DNA cross-linked products (**20**) possibly due to its disrupted conjugation system (Scheme 4 and SI, Figure S7). The fast and quantitative formation of a nonfluorescent ICL product from a highly fluorescent coumarin moiety encourages us to develop a novel method for detecting DNA cross-linking using a fluorescence assay. We observed that the fluorescence of ds DNA-**4** decreased steadily upon ICL

Scheme 4. Mechanism of ICL Formation

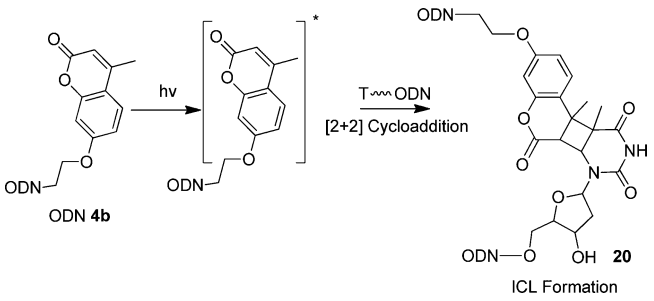

formation via 350 nm irradiation (Figure 5a). Almost no fluorescence was detected when 98% ICL was produced with 10 μM ds DNA-**4** upon 60 min irradiation at 350 nm (Figures 3 and 5a). As the ICL product is nonfluorescent, the fluorescence intensity observed in the reaction mixture results from the unreacted DNA duplexes. It is well-known that the fluorescence intensity is linearly correlated with the fluorophore concentration at the μM level (self-quenching could occur at high concentration of mM level).[36] Based on these facts, a reasonable equation ICL yield = $[I_0 - I/I_0 - I_{60}]$* 98% was proposed, where I_0 is the fluorescence intensity of unreacted ds DNA-**4** at 0 min, I is the fluorescence intensity of ds DNA-**4** upon photoirradiation for the desired time, I_{60} is the fluorescence intensity of ds DNA-**4** upon photoirradiation for 60 min. The rate constants determined by fluorescence assay ($k_{cal.\text{-}4}$ (4.66 ± 0.27) × 10^{-3} s^{-1}) were within the experimental error of those measured using ^{32}P-labeling method ((5.04 ± 0.38) × 10^{-3} s^{-1}) (Figure 5b and Table 2). The reliability of this method was further examined by measuring the rate constants of ICL formation with ds DNA-**7**–**9** using fluorescence assay (Table 2 and SI, Figures S8–10). The data

dx.doi.org/10.1021/jo5014756 | J. Org. Chem. XXXX, XXX, XXX–XXX

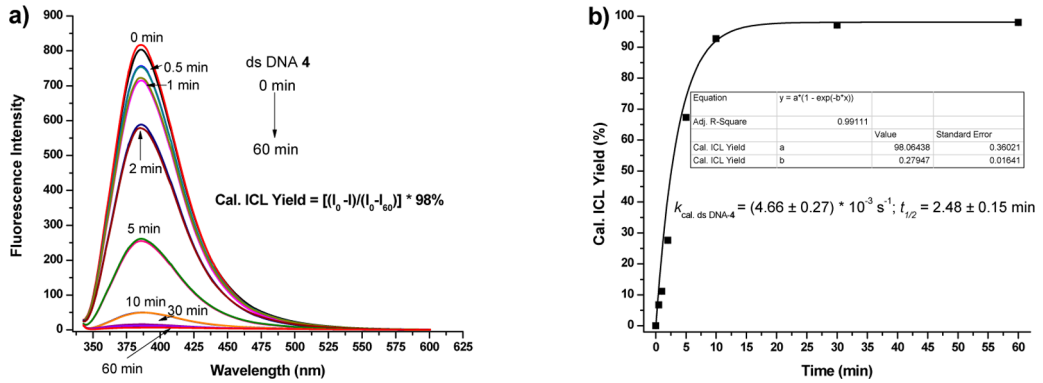

Figure 5. Determination of ICL formation rate constant via fluorescence assay: (a) fluorescence emission spectra of two independent samples containing 10 μM ds DNA-**4** which were irradiated at 350 nm for the desired time (λ_{ex} = 325 nm, slit width = 15 nm; λ_{em} = 385 nm, slit width = 10 nm); (b) rate of DNA cross-linking formation.

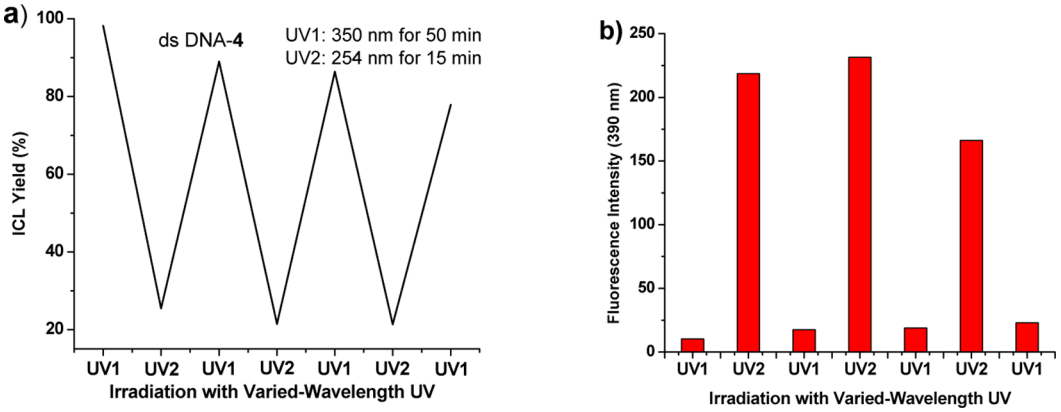

Figure 6. Photoreversible process for ds DNA-**4** over three cycles of photoirradiation at 350 nm for 50 min (UV1) and 254 nm (UV2) for 15 min: (a) ICL yields obtained from phosphorimage autoradiogram of denaturing PAGE analysis of 100 nM ds DNA-**4** (ODN **1a** was 5′-[^{32}P]-labeled); (b) fluorescence intensity at 390 nm of 10 μM ds DNA-**4** (λ_{ex} = 325 nm, slit width = 15 nm; λ_{em} = 390 nm, slit width = 10 nm).

obtained from the fluorescence assay are consistent with those obtained by ^{32}P-labeling method (Table 2). This is the first example that allows rapid, direct, and efficient monitoring of the DNA cross-linking process on time via a noninvasive method instead of employing a traditionally used harmful ^{32}P-labeling method in biochemical research. The novel method could be introduced as an effective way in biology for DNA cross-linking study and allowing real-time detection without disrupting native cell environment.

Photoreversibility. The ICL formation induced by coumarin moiety is photoreversible. The DNA cross-linked products generated by 350 nm irradiation were split into single-stranded ODNs upon irradiation at 254 nm for 15 min. Initially, we observed the decomposition of dT-coumarin dimers (**17** and **18**) to coumarin **1** and thymidine during HRMS mass measurement, which indicated that [2 + 2] cycloaddition products were cleaved into starting materials upon high voltage electrons. Later, we found that **17** and **18** were cleaved by 254 nm irradiation, which was confirmed by NMR analysis (SI, Figure S11). Cleavage reaction was also observed with DNA cross-linked products formed with ds DNA-**4** and **7**−**9** upon irradiation at 254 nm. The cleavage of the ICL products followed first-order kinetics and the rate for cleavage reaction is sequence-dependent. The G:C base pair flanking to the cross-linking site led to a faster cleavage reaction than an A:T base pair (ds DNA-**8** and **9** vs ds DNA-**4** and **7**) (Table 2 and SI, Figures S12−13). This reversible behavior was observed over three cycles of photo irradiation at 350 nm for 50 min and 254 nm for 15 min (Figure 6). The efficient ICL formation (around 80% ICL yield) was still achieved after three cycles of 350 nm/254 nm irradiation (Figure 6a and SI, Figure S14b). The photoswitchable ICL formation can be monitored by fluorescence spectroscopy. Irradiation of ds DNA-**4** at 350 nm quenches the fluorescence due to formation of cyclobutane product **20**, while 254 nm irradiation cleaves **20** to a single-stranded ODN which greatly enhanced the fluorescence intensity (Figure 6b). A similar result was observed for ds DNA-**7** indicating its generality (SI, Figures S14a and S15).

Fluorescence Detection of Single Nucleotide Discrimination. Different reactivities of coumarin toward canonical nucleosides and fluorescence quenching induced by ICL formation encouraged us to use this reaction for detecting single nucleotide polymorphisms (SNPs) via fluorescence assay. As purines decrease the activity and fluorescence intensity of coumarin, we expect that a method based on coumarin cross-linking can be developed for detecting transversion of pyrimidines to purines and vice versa. A probe ODN **11** containing coumarin moiety **4** and templates ODNs **11a**−**c** were designed for this study. The templates contain sequences of codon 248 in exon 7 of the p53 gene, which are often mutated in human cancers. ODN **11a** contains the wild-type genetic sequence with dT at the 3′-termius, while ODN **11b** and **11c** contain a T → A or G transversion mutation. Upon photoirradiation at 350 nm for 1 h, a much

dx.doi.org/10.1021/jo5014756 | J. Org. Chem. XXXX, XXX, XXX−XXX

higher cross-linking yield was observed for ds DNA-**11a** (92%) than ds DNA-**11b** (8%) and **11c** (6%) (SI, Figure S16a). The different cross-linking efficiency was also detected via fluorescence assay. The fluorescence intensity was significantly decreased with DNA-**11a** upon 350 nm irritation for 1 h, while a much lower decrease was observed for DNA-**11b** and DNA-**11c** (SI, Figure S16b). The decreased fluorescence intensity after UV irradiation for 1 h is shown in Figure 7. Obviously,

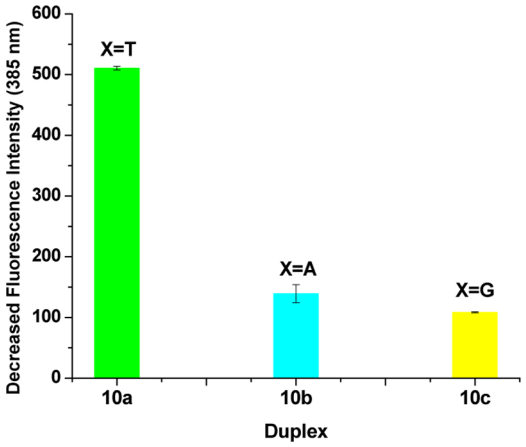

Figure 7. Decreased fluorescence intensity at 385 nm after UV irritation at 350 nm for 1 h with 10 μM ds DNA-**11a**−**c** (λ_{ex} = 325 nm, slit width = 6 nm; λ_{em} = 385 nm, slit width = 14 nm).

such a reaction can be directly used to monitor a T → A or G transversion and vice versa. In addition, ICL formation with ds DNA-**11a** ($(9.17 \pm 1.01) \times 10^{-4}$ s^{-1}) is about 8−11 times faster than those for ds DNA-**11b** ($(8.3 \pm 0.9) \times 10^{-5}$ s^{-1}) and **11c** ($(9.7 \pm 0.8) \times 10^{-5}$ s^{-1}) (SI, Table S1 and Figures S17−18). In this way, coumarin-containing DNAs may have the potential to detect T↔A or G transversion via fluorescence assay.

Effect of the Modification Site and the Template Length on Coumarin-dT Cross-Linking. To explore the generality and versatility of the photoswitchable DNA cross-linking induced by coumarin moieties, we performed the same type of experiments using a diol-based coumarin **7** which was incorporated into ODNs at two different internal positions (**10b** and **13b**). Similar to a terminal coumarin, compound **7** at the internal position (ds DNA-**10**) lead to almost quantitative ICL formation (97%) upon photoirradiation at 350 nm (Figure 8, lane 2). The DNA cross-linking product formed with ds DNA-**10** was split into single-stranded ODNs upon 254 nm irradiation with good efficiency (cleavage percentage 84%) (Figure 8, lane 3). Kinetic study showed that both ICL formation and cleavage reactions were very fast and finished with 10 min (Table 3, and SI, Figures S19a, 20a, 21a, and 22a).

Table 3. Rate of ICL Formation or Cleavage of ds DNA-10, 12, and 13

entry	k (ICL Formation, 10^{-3} s^{-1})	$t_{1/2}$ (min)	k_c (Cleavage, 10^{-2} s^{-1})	$t_{1/2}$ (min)
ds DNA-**10**	3.99 ± 0.32	2.91 ± 0.23	0.57 ± 0.04	2.02 ± 0.13
ds DNA-**12**	6.27 ± 0.62	1.86 ± 0.18	1.67 ± 0.19	0.70 ± 0.08
ds DNA-**13**	1.55 ± 0.14	7.51 ± 0.66	1.42 ± 0.03	0.82 ± 0.02

After having established the chemistry and the generality of the photoswitchable DNA interstrand cross-linking by coumarin moieties, we investigated their reactivities toward a longer DNA template which provides a more realistic illustration of how these molecules might perform in cellular DNA. We studied the reactivity of a terminal coumarin (**4** in ODN **7b**) as well as an internal coumarin (**7** in ODN **13b**) toward dT in a 50-mer ODN template **12a**. Almost quantitative DNA cross-link formation was observed for **4** in ds DNA-**12** (98%, Figure 8, lane 5) upon 350 nm irradiation and compound **7** in ds DNA-**13** also lead to a reasonable ICL yield (84%, Figure 8, lane 8). The cross-linked products formed with ds DNA-**12** and **13** efficiently reverted to the single-stranded ODNs upon 254 nm irradiation (Figure 8, lanes 6 and 9). The cleavage reactions proceeded at a faster rate compared with when a shorter ODN template was used, such as ds DNA-**10** (Table 3, and SI, Figures S21−22). The generality and template versatility of photoswitchable coumarin-dT cross-linking provide a powerful and versatile tool for expanding its bioapplication.

CONCLUSION

A series of coumarin analogues (**2**−**7**) with varied modifications at the position-4 or -7 have been synthesized and successfully incorporated into oligonucleotides. Coumarin analogues increase the DNA duplex stability. Coumarin scaffolds undergo photoinduced [2 + 2] cycloaddition with thymidine and form *syn*- and *anti*-cyclobutane adducts (**17** and **18**) which were confirmed by NMR as well as mass analysis. The photocyclization reaction between coumarin and thymidine leads to fast and quantitative DNA interstrand cross-link formation with a 2.3 min half-life. A two-carbon or longer chain linker at the position-7 of coumarin moiety (**4** and **5**) is optimal for quantitative DNA cross-linking formation (>98%). Flanking sequences greatly affect the cross-linking efficiency and rate constant, as well as the fluorescence intensity of the coumarin

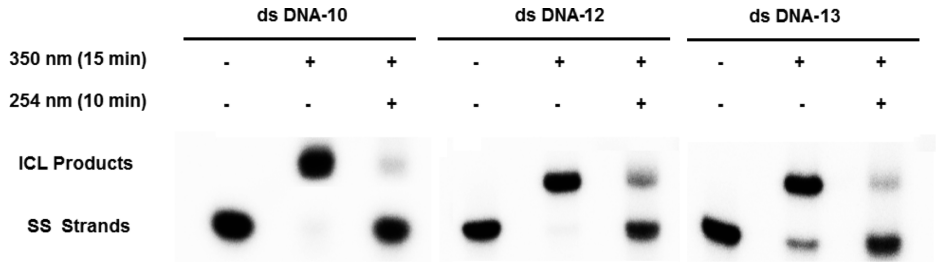

Figure 8. Phosphorimage autoradiogram of denaturing PAGE analysis of ICL formation and cleavage of ds DNAs-**10**, **12**, and **13** (100 nM ds DNA were irradiated at 350 or 254 nm; ODNs without coumarin were 5′-[^{32}P]-labeled).

dx.doi.org/10.1021/jo5014756 | J. Org. Chem. XXXX, XXX, XXX−XXX

moiety. The cross-linking formation induced by a coumarin moiety flanked by a G:C pair is 10 times slower than when coumarin is adjacent to an A:T base pair. This is caused by the large difference of the redox potential between coumarin (2.10 V) and dG (1.25 V) leading to an efficient electron transfer.

The ICL formation induced by coumarin moieties is highly reversible. The DNA cross-linked products generated by 350 nm irradiation can be reverted to the single-stranded ODNs by 254 nm irradiation while 80% cross-linking yield was still obtained even after 3 cycles. Most importantly, ICL formation completely quenches the fluorescence of coumarin, which allows for the monitoring of DNA cross-linking process on time via fluorescence spectroscopy. To the best of our knowledge, this is the first example that DNA interstrand cross-linking can be directly quantitated using fluorescence spectroscopy. This methodology also allows us to detect DNA transversion mutation between pyrimidines and purines with a good discriminating effect. Overall, coumarin analogues developed in this work provide a means of fast, quantitative, directly detectable, and photoswitchable DNA cross-linking, which could serve as mechanistic probes and tools for bioresearch.

EXPERIMENTAL SECTION

General Methods. Unless otherwise specified, reagents were used as received without further purification. T4 polynucleotide kinase was purchased from New England Biolabs. [γ-^{32}P]-ATP was obtained from PerkinElmer Life Sciences. ODNs were synthesized via standard automated DNA synthesis techniques in a 1.0 μmol scale using commercial 1000 Å CPG-succinyl-nucleoside supports. The ^{i}Pr-Pac-dA and ^{i}Pr-Pac-dG phosphoramidites were employed for the synthesis of coumarin-containing ODNs. Deprotection of the nucleobases and phosphate moieties as well as cleavage of the linker for normal ODNs were carried out with a mixture of 40% aq. $MeNH_2$ and 28% aq. NH_3 (1:1) at room temperature for 2 h. Functional ODNs were deprotected and cleaved using 28% aq. NH_3 at room temperature for 2 h. Crude ODNs were purified by 20% denaturing polyacrylamide gel electrophoresis (PAGE) analysis, and quantified in water by UV–vis spectrophotometer at 260 nm. Thermal denaturation temperatures (T_m) were measured via changing temperature of DNA duplex at a rate of 1 °C/min on a UV/vis sepectrometer equipped with a thermoelectrical temperature controller. Radiolabeling was carried out according to the standard protocols. The ^{32}P-labeled ODN (100 nM) was annealed with 1.5 equiv of the complementary strand by heating to 80 °C for 3 min in a buffer of 10 mM potassium phosphate (pH 7.0) and 100 mM NaCl, followed by slow-cooling to room temperature overnight. Quantification of radiolabeled ODNs was carried out using a Molecular Dynamics Phosphorimager equipped with ImageQuant v 5.2 software.

Photoirradiation at 350 nm was conducted in Rayonet Photochemical Chamber Reactor. Fluorescence spectra were recorded using the quartz cell with 10 mm path lengths at room temperature. Compounds **1**, **2**, **4**, **5**, and **7** were synthesized with modified procedures.[37,38] ^{1}H NMR, ^{13}C NMR, and ^{31}P NMR analysis were performed on a 300 MHz spectrophotometer. Chemical shifts are reported in ppm relative to Me_4Si (^{1}H and ^{13}C) or H_3PO_4 (^{31}P). Coupling constants (J) are reported in Hz. High resolution MALDI-TOF-MS spectrometry was performed at the University of California-Riverside Mass Spectrometry Lab.

LC-MS Analysis of Photoinduced Reaction between Coumarin 1 and Canonical Nucleosides. The reaction mixtures containing 30 nmol deoxyribonucleosides (dA: 7.5 mg, dT: 7.2 mg, dG: 8.0 mg, or dC: 6.8 mg) and coumarin **1** (5.7 mg, 30 nmol) in methanol (1–6 mL, depending on solubility) were placed in four vials, respectively. After UV irradiation at 350 nm for 2 days, the mixtures were diluted to the desired concentration for LC-MS analysis.

Preparation of DNA Cross-Linked Products for MALDI-TOF-MS Analysis. Interstrand cross-linking reactions were performed using 10 μM coumarin-containing oligonucleotides, which were annealed with 1.0 equiv of the complementary strands by heating to 80 °C for 3 min in a buffer containing 10 mM pH 7 potassium phosphate buffer and 100 mM NaCl, followed by slowly cooling to room temperature overnight. The DNA duplexes were irradiated with the UV light at 350 nm for the desired time to make sure that the reactions were complete. Then, 2 M NaCl solution (200 μL) and cold ethanol (1.2 mL) were added to the reaction mixture which was incubated at −80 °C for 30 min. ODNs were precipitated by centrifugation at 15 000 g for 6 min at room temperature. The crude DNA was further purified via C18 column eluting with H_2O (3 × 1.0 mL) followed by MeOH:H_2O (3:2, 1.0 mL) to remove salts. The afforded ODNs were dried and characterized by MALDI-TOF-MS at the University of California-Riverside Mass Spectrometry Lab.

Determination of DNA Duplexes' Thermal Stability. All measurements were carried out in 10 mM potassium phosphate buffer (pH 7), 100 μM ethylenediaminetetraacetic acid (EDTA), and 100 mM NaCl, with 4 μM + 4 μM single-strand concentration. Samples were heated at 1 °C min^{-1} from 20 to 80 °C and the absorbance of DNA at 260 nm was measured at 1.0 °C steps. At least two independent samples have been tested to get the melting temperatures of DNA duplexes.

PAGE Analysis of Interstrand Cross-Link Formation and Kinetic Study using ^{32}P-Labeling Method. ODNs (0.1 μM) without coumarin were 5′-^{32}P-labeled and hybridized with 1.5 equiv of the complementary strands in 100 mM NaCl and 10 mM potassium phosphate (pH 7). The DNA duplexes were irradiated at 350 nm to form ICLs (a control reaction was carried out without photoirradiation). Aliquots were taken at the prescribed time and immediately quenched with the equal volume of 95% formamide loading buffer, and stored at −20 °C until subjecting to 20% denaturing PAGE analysis. For kinetics study, three independent samples were used with the same procedures mentioned above.

Kinetic Study of DNA Interstrand Cross-Link Formation using Fluorescence Assay. Coumarin-modified ODNs (10 μM) were hybridized with 1.0 equiv of the complementary strands in 100 mM NaCl and 10 mM potassium phosphate (pH 7). The DNA duplexes were irradiated at 350 nm and the fluorescence was measured at the prescribed time. The equations used for calculation of the ICL yields were shown in each figure. For kinetics study, two independent samples were used.

PAGE Analysis of Photo-Induced (254 nm) Cleavage Reactions of DNA ICL Products and Kinetic Study. The reactions were carried out with photoirradiation at 254 nm using two or three independent samples. Aliquots were taken at the prescribed time and immediately quenched with the equal volume of 95% formamide loading buffer, and stored at −20 °C until subjected to 20% denaturing PAGE analysis.

7-Hydroxy-4-methyl-2*H*-chromen-2-*O*-(2-cyanoethyl-*N*,*N*-diisopropyl)-phosphoramidite (8). To a solution of 7-hydroxy-4-methyl-2*H*-chromen-2-one (**3**, 88 mg, 0.5 mmol) in dichloromethane (10 mL), *N*,*N*-diisopropylethylamine (DIPEA) (156 μL, 0.9 mmol), and 2-cyanoethyl-*N*,*N*-diisopropylchlorophosphoramidite (167 μL, 0.75 mmol) were added under an atmosphere of argon. The reaction mixture was stirred at room temperature for 3 h and diluted with dichloromethane (50 mL). The organic layer was washed with $NaHCO_3$ (20 mL) and saturated aqueous NaCl (20 mL), and dried over anhydrous sodium sulfate. The solvent was removed under reduced pressure. Upon purification by column chromatography (EtOAc:hexane:Et_3N = 59:40:1), the product was isolated as a white solid (**8**, 170 mg, 90%). ^{31}P NMR (300 MHz, $CDCl_3$-d): δ 147.48. ^{1}H NMR (300 MHz, $CDCl_3$-d): δ 7.50–7.53 (m, 1H), 7.00–7.02 (dd, J = 1.5 Hz, 2H), 6.18 (s, 1H), 3.93–4.01 (m, 2H), 3.71–3.79 (m, 2H), 2.69–2.73 (t, J = 6.3 Hz, 3H), 1.18–1.27 (dd, J = 6.6 Hz, 1H). ^{13}C NMR (300 MHz, $CDCl_3$-d): δ 161.1, 157.7, 157.6, 154.8, 152.4, 125.5, 117.3, 116.5, 116.4, 115.0, 112.7, 107.5, 107.3, 59.3, 59.0, 44.0, 43.8, 24.7, 24.6, 24.5, 24.4, 20.4, 20.3, 18.7. HRMS-ESI (+) (m/z): [M + H]$^+$ calcd. for $C_{19}H_{26}N_2O_4P$, 377.1625; found: 377.1633.

4-Methyl-7-methoxy-2*H*-chromen-2-one (1). Iodomethane (1.3 mL, 20 mmol) was added to a suspension of 7-hydroxy-4-

dx.doi.org/10.1021/jo5014756 | J. Org. Chem. XXXX, XXX, XXX–XXX

methyl-2*H*-chromen-2-one (**3**, 704 mg, 4 mmol) and K_2CO_3 (600 mg, 3.34 mmol) in acetone (50 mL). The reaction mixture was stirred at 50 °C overnight. After cooling to room temperature, the solvent was removed under reduced pressure. The residue was diluted with ethyl acetate (50 mL), washed with 1 M HCl (30 mL), H_2O (30 mL), and brine (20 mL), and then dried over anhydrous sodium sulfate. The solvent was removed under vacuum providing the product **1** as a white solid (699 mg, 92%). ^{1}H NMR (300 MHz, $CDCl_3$-*d*): δ 7.60−7.65 (m, 1H), 7.01−7.02 (t, J = 1.8 Hz, 1H), 6.93−6.98 (m, 2H), 6.25, 6.28 (t, J = 1.8 Hz, 1H), 3.86 (s, 3H), 2.37 (s, 3H).

4-(Hydroxymethyl)-7-methoxy-2*H*-chromen-2-one (2). To a suspension of 7-hydroxy-4-(hydroxylmethyl)-2*H*-chromen-2-one (**14**, 384 mg, 2 mmol) and K_2CO_3 (300 mg, 2.17 mmol) in acetone (30 mL), iodomethane (0.65 mL, 10 mmol) was added. The reaction mixture was stirred at 50 °C overnight. After cooling to room temperature, the solvent was removed under reduced pressure. The residue was diluted with ethyl acetate (50 mL), washed with 1 M HCl (30 mL), and brine (20 mL), and then dried over anhydrous sodium sulfate. The solvent was removed under vacuum providing **2** as a white solid (394 mg, 96%). ^{1}H NMR (300 MHz, $CDCl_3$-*d*): δ 7.61−7.64 (m, 1H), 7.01−7.02 (t, J = 1.8 Hz, 1H), 6.92−6.97 (m, 1H), 6.30, 6.31 (t, J = 1.5 Hz, 1H), 5.60−5.64 (m, 1H), 4.73−4.75 (t, J = 1.5 Hz, 2H), 3.85, 3.86 (d, J = 1.8 Hz, 3H).

4-(Hydroxymethyl)-7-methoxy-2*H*-chromen-2-*O*-(2-cyanoethyl-*N*,*N*-diisopropyl)-phosphor-amidite (9). Compound **2** (103 mg, 0.5 mmol) was dissolved in dichloromethane (8 mL) under an atmosphere of argon. *N*,*N*-Diisopropylethylamine (DIPEA) (156 μL, 0.9 mmol) was then added dropwise, followed by 2-cyanoethyl-*N*,*N*-diisopropylchlorophosphoramidite (167 μL, 0.75 mmol). The reaction mixture was stirred at room temperature for 3 h, then diluted by dichloromethane (30 mL), washed with $NaHCO_3$ (20 mL), and brine (20 mL), and dried over anhydrous sodium sulfate. The solvent was removed under reduced pressure. Upon purification by column chromatography (EtOAc:hexane:Et_3N = 40:59:1), the product **9** was isolated as a white solid (148 mg, 73%). ^{31}P NMR (300 MHz, $CDCl_3$-*d*): δ 149.96. ^{1}H NMR (300 MHz, $CDCl_3$-*d*): δ 7.44−7.47 (m, 1H), 6.84−6.88 (dd, J = 3.0 Hz, 2H), 6.44−6.45 (d, J = 1.5 Hz, 1H), 4.84−4.90 (m, 2H), 3.85−3.95 (m, 5H), 3.68−3.71 (dd, J = 3.6 Hz, 2H), 2.66−2.71 (t, J = 6.3 Hz, 2H), 1.22−1.25 (dd, J = 2.4 Hz, 12H). ^{13}C NMR (300 MHz, $CDCl_3$-*d*): δ 162.6, 161.5, 155.4, 152.5, 152.4, 124.5, 117.6, 112.4, 110.9, 109.5, 101.1, 61.7, 61.5, 58.5, 58.2, 55.8, 43.5, 43.3, 24.8, 24.7, 24.6, 20.5, 20.4. HRMS-ESI (+) (m/z): $[M + H]^+$ calcd. for $C_{20}H_{28}N_2O_5P$, 407.1730; found: 407.1745.

7-(2-Hydroxyethoxy)-4-methyl-2*H*-chromen-2-one (4). To a suspension of 7-hydroxy-4-methyl-2*H*-chromen-2-one (**3**, 704 mg, 4 mmol), KI (1.65 g, 10 mmol), and K_2CO_3 (900 mg, 6.51 mmol) in acetone (60 mL), 2-bromoethanol (1.42 mL, 20 mmol) was added. The reaction mixture was stirred at 50 °C for 48 h. After cooling to room temperature, the solvents were removed under reduced pressure. The residue was diluted with ethyl acetate (80 mL), washed with 1 M HCl (40 mL), and brine (20 mL), and then dried over anhydrous Na_2SO_4. The solvent was removed under reduced pressure. The crude product was purified by column chromatography (EtOAc) yielding **4** as a white solid (642 mg, 73%). ^{1}H NMR (300 MHz, $CDCl_3$-*d*): δ 7.67, 7.70 (d, J = 9.3 Hz, 1H), 6.96, 6.99 (d, J = 6.6 Hz, 2H), 6.21 (s, 1H), 4.90−4.93 (t, J = 5.4 Hz, 1H), 4.09−4.12 (t, J = 5.4 Hz, 2H), 3.72−3.77 (dd, J = 5.1 Hz, 2H), 2.40 (s, 3H).

7-(3-Hydroxypropoxy)-4-methyl-2*H*-chromen-2-one (5). To a suspension of **3** (704 mg, 4 mmol), KI (1.65 g, 10 mmol), and K_2CO_3 (900 mg, 6.51 mmol) in acetone (60 mL), 3-bromo-1-propanol (0.54 mL, 6 mmol) was added. The reaction mixture was stirred at 50 °C for 36 h. After cooling to room temperature, the solvent was removed under reduced pressure. The residue was diluted with ethyl acetate (80 mL), washed with 1 M HCl (40 mL), and brine (20 mL), and then dried over anhydrous Na_2SO_4. The solvent was removed under reduced pressure to afford **5** as a white solid (760 mg, 81%). ^{1}H NMR (300 MHz, $CDCl_3$-*d*): δ 7.49, 7.52 (d, J = 8.7 Hz, 1H), 6.83−6.90 (m, 2H), 6.14 (s, 1H), 4.18−4.22 (t, J = 6.0 Hz, 2H), 3.87−3.92 (dd, J = 5.4 Hz, 2H), 2.41 (s, 3H), 2.06−2.14 (m, 2H).

7-(2-Hydroxyethoxy)-4-methyl-2*H*-chromen-2-*O*-(2-cyanoethyl-*N*,*N*-diisopropyl)-phosphoramidite (10). To a solution of **4** (110 mg, 0.5 mmol) in dichloromethane (10 mL), *N*,*N*-diisopropylethylamine (DIPEA) (156 μL, 0.9 mmol) and 2-cyanoethyl-*N*,*N*-diisopropylchlorophosphoramidite (167 μL, 0.75 mmol) were added under an atmosphere of argon. The reaction mixture was stirred at room temperature for 3 h and diluted with EtOAc (50 mL). The organic layer was washed with $NaHCO_3$ (20 mL) and saturated aqueous NaCl (20 mL), and dried over anhydrous sodium sulfate. The solvent was removed under reduced pressure. The crude product was purified by column chromatography (EtOAc:hexane:Et_3N = 49:50:1) yielding **10** as a white solid (162 mg, 77%). ^{31}P NMR ($CDCl_3$-*d*, 300 MHz): δ 149.28. ^{1}H NMR ($CDCl_3$-*d*, 300 MHz): δ 7.41, 7.44 (d, J = 8.7 Hz, 1H), 6.75−6.82 (t, J = 8.7 Hz, 2H), 6.06 (s, 1H), 4.12−4.15 (t, J = 4.5 Hz, 2H), 3.88−4.00 (m, 2H), 3.75−3.80 (m, 2H), 3.52−3.60 (m, 2H), 2.55−2.59 (t, J = 6.3 Hz, 2H), 2.32 (s, 3H), 1.11, 1.13 (d, J = 6.6 Hz, 12H). ^{13}C NMR (300 MHz, $CDCl_3$-*d*): δ 161.8, 161.2, 155.2, 152.6, 125.6, 117.6, 113.7, 112.6, 112.0, 101.6, 68.6, 68.5, 61.9, 61.6, 58.6, 43.2, 43.1, 24.7, 24.6, 20.4, 20.3, 18.7. HRMS-ESI (+) (m/z): $[M + H]^+$ calcd. for $C_{21}H_{30}N_2O_5P$, 421.1887; found: 421.1899.

7-(3-Hydroxypropoxy)-4-methyl-2*H*-chromen-2-*O*-(2-cyanoethyl-*N*,*N*-diisopropyl)-phosphoramidite (11). To a solution of **5** (117 mg, 0.5 mmol) in dichloromethane (10 mL), *N*,*N*-diisopropylethylamine (DIPEA) (156 μL, 0.9 mmol) and 2-cyanoethyl-*N*,*N*-diisopropylchlorophosphoramidite (167 μL, 0.75 mmol) were added under an atmosphere of argon. The reaction mixture was stirred at room temperature for 3 h and diluted with dichloromethane (30 mL). The organic layer was washed with $NaHCO_3$ (20 mL) and saturated aqueous NaCl (20 mL), and dried over anhydrous sodium sulfate. The solvent was removed under reduced pressure. The residue was purified by column chromatography (EtOAc:hexane:Et_3N = 49:50:1) providing **11** as a white solid (120 mg, 55%). ^{31}P NMR ($CDCl_3$-*d*, 300 MHz): δ 147.89. ^{1}H NMR ($CDCl_3$-*d*, 300 MHz): δ 7.40, 7.43 (d, J = 8.7 Hz, 1H), 6.75−6.81 (m, 2H), 6.06 (s, 1H), 4.06−4.10 (t, J = 6.0 Hz, 2H), 3.72−3.80 (m, 2H), 3.49−3.57 (m, 2H), 2.33 (s, 3H), 2.03−2.07 (t, J = 6.0 Hz, 2H), 1.10, 1.11 (t, J = 2.1 Hz, 12H). ^{13}C NMR (300 MHz, $CDCl_3$-*d*): δ 162.1, 161.3, 155.3, 152.5, 125.5, 117.6, 113.6, 112.6, 111.9, 101.5, 65.1, 60.0, 59.8, 58.4, 58.2, 43.2, 43.0, 30.8, 30.7, 24.7, 24.6, 20.4, 20.3, 18.7. HRMS-ESI (+) (m/z): $[M + H]^+$ calcd. for $C_{22}H_{32}N_2O_5P$, 435.2043; found: 435.2055.

7-(1-(3-Hydroxypropyl)-1*H*-1,2,3-triazol-5-yl)-4-methyl-2*H*-chromen-2-one (6). To a suspension of 7-ethynyl-4-methyl-2*H*-chromen-2-one (**15**, 184 mg, 1 mmol), 3-azidopropan-1-ol (152 mg, 1.5 mmol) and copper(II) sulfate (pentahydrate) (50 mg, 0.2 mmol) in a mixture of water (10 mL) and *tert*-butyl alcohol (10 mL), sodium ascorbate (119 mg, 0.6 mmol) was added and stirred at room temperature overnight. After addition of water (20 mL) to mixture, extract with ethyl acetate (20 mL × 3). The organic phases were collected, washed with water (20 mL × 2) and brine (20 mL), and then dried over anhydrous Na_2SO_4. The solvent was removed under reduced pressure and the white residue was purified by column chromatography (EtOAc) to afford **6** as a white solid (186 mg, 65%). ^{1}H NMR (300 MHz, $CDCl_3$-*d*): δ 8.79 (s, 1H), 7.81−7.86 (m, 3H), 6.39 (s, 1H), 4.70−4.73 (t, J = 5.1 Hz, 1H), 4.47−4.52 (t, J = 6.9 Hz, 2H), 3.43−3.49 (dd, J = 6.0 Hz, 2H), 2.45 (s, 3H), 2.00−2.08 (m, 2H). ^{13}C NMR (300 MHz, $CDCl_3$-*d*): δ 160.2, 154.0, 153.5, 145.3, 134.8, 126.6, 123.4, 121.4, 119.4, 114.5, 57.9, 47.5, 33.2, 18.5. HRMS-ESI (+) (m/z): $[M + H]^+$ calcd. for $C_{15}H_{16}N_3O_3$, 286.1192; found: 286.1186.

2-Cyanoethyl (3-(4-(4-methyl-2-oxo-2*H*-chromen-7-yl)-1*H*-1,2,3-triazol-1-yl)propyl) diisopropyl-phosphoramidite (12). To a suspension of **6** (143 mg, 0.5 mmol) in dichloromethane (10 mL), *N*,*N*-diisopropylethylamine (DIPEA) (156 μL, 0.9 mmol) and 2-cyanoethyl-*N*,*N*-diisopropylchlorophosphoramidite (167 μL, 0.75 mmol) were added under an atmosphere of argon. The reaction mixture was protected from light by aluminum foil, stirred at room temperature for 3 h, and diluted with dichloromethane (30 mL). The organic layer was washed with 1 M $NaHCO_3$ (20 mL) and saturated

dx.doi.org/10.1021/jo5014756 | J. Org. Chem. XXXX, XXX, XXX−XXX

aqueous NaCl (20 mL), and dried over anhydrous sodium sulfate in the dark room. The solvent was removed under reduced pressure. The crude product was purified by column chromatography (EtOAc:hexane:Et_3N = 49:50:1) in the dark room yielding **12** as a white solid (73 mg, 30%). ^{31}P ($CDCl_3$-*d*, 300 MHz): δ 148.06. ^1H NMR ($CDCl_3$-*d*, 300 MHz): δ 7.92 (s, 1H), 7.76−7.78 (d, J = 8.1 Hz, 1H), 7.63 (s, 1H), 7.56−7.58 (d, J = 8.4 Hz, 1H), 6.19 (s, 1H), 4.49−4.54 (t, J = 6.9 Hz, 2H), 3.48−3.86 (m, 6H), 2.57−2.61 (t, J = 6.0 Hz, 2H), 2.38 (s, 3H), 2.20−2.24 (t, J = 6.0 Hz, 2H), 1.09−1.13 (dd, J = 4.2 Hz, 12H). ^{13}C NMR (300 MHz, $CDCl_3$-*d*): δ 159.8, 152.9, 151.2, 144.9, 133.4, 124.2, 120.5, 118.5, 116.8, 113.8, 112.5, 59.0, 58.8, 57.4, 57.1, 46.3, 42.2, 42.0, 30.6, 30.5, 23.7, 23.6, 19.6, 19.5, 17.6. HRMS-ESI (+) (m/z): $[M + H]^+$ calcd. for $C_{24}H_{33}N_5O_4P$, 486.2278; found: 486.2285.

7-(2,3-Dihydroxypropoxy)-4-methyl-2*H*-chromen-2-one (7). To a suspension of 7-hydroxy-4-methyl-2*H*-chromen-2-one (**3**, 1.76 g, 10 mmol) and KOH (1.12 g, 20 mmol) in ethanol (50 mL), epichlorohydrin (8.0 mL, 102 mmol) and KI (166 mg, 1 mmol) were added. The reaction mixture was stirred at 70 °C overnight. After cooling to room temperature, the solvent was removed under vacuum. The residue was submitted to flash chromatography (CH_2Cl_2:MeOH = 98:2) to afford 4-methyl-7-(oxiran-2-ylmethoxy)-2*H*-chromen-2-one as a white solid (1.83 g, 79%). ^1H NMR (300 MHz, $CDCl_3$-*d*): δ 7.42−7.45 (d, J = 9.0 Hz, 1H), 6.81−6.85 (dd, J = 2.4 Hz, 1H), 6.76 (d, J = 2.4 Hz, 1H), 6.08 (s, 1H), 4.25−4.29 (d, J = 2.7 Hz, 1H), 3.88−3.93 (q, J = 6.0 Hz, 1H), 3.30−3.35 (m, 1H), 2.86−2.89 (t, J = 4.5 Hz, 1H), 2.71−2.74 (q, J = 2.7 Hz, 1H), 2.33 (s, 3H). The solution of 4-methyl-7-(oxiran-2-ylmethoxy)-2*H*-chromen-2-one (1.16 g, 5 mmol) in 6% perchloric acid (40 mL) was stirred at room temperature overnight. Then, the pH of the solution was adjusted to 8 via addition of Na_2CO_3. After stirring for 2 h, ethyl acetate (80 mL) was added and stirred for 20 h. The organic layer was washed with water (20 mL) and saturated aqueous NaCl (20 mL), and dried over anhydrous sodium sulfate. The solvent was removed under reduced pressure to afford **7** (1.05 g, 84%) as a viscous liquid which was easily solidified into a white solid at room temperature. ^1H NMR (DMSO-d_6): δ 7.66−7.68 (d, J = 8.4 Hz, 1H), 6.95−6.99 (m, 2H), 6.20 (s, 1H), 5.04−5.06 (d, J = 5.1 Hz, 1H), 4.72−4.76 (t, J = 5.4 Hz, 1H), 4.10−4.14 (dd, J = 3.9 Hz, 1H), 3.96−4.01 (m, 1H), 3.80−3.85 (m, 1H), 3.44−3.48 (t, J = 5.4 Hz, 2H), 3.04 (s, 3H).

7-(3-(Bis(4-methoxyphenyl)(phenyl)methoxy)-2-hydroxypropoxy)-4-methyl-2*H*-chromen-2-one (16). To a solution of compound **7** (0.50 g, 2.0 mmol) in pyridine (8 mL), 4,4′-dimethoxytriphenylmethyl chloride (0.81 g, 2.4 mmol) was added. The mixture was stirred at room temperature overnight. The reaction mixture was quenched with MeOH (5 mL) and concentrated under reduced pressure. Upon purification by column chromatography (EtOAc:Et_3N = 99:1), **16** was isolated as a white foam (0.76 g, 69%). ^1H NMR (DMSO-d_6): δ 7.67−7.70 (d, J = 8.7 Hz, 1H), 7.39−7.41 (d, J = 7.5 Hz, 2H), 7.19−7.32 (m, 7H), 6.85−6.96 (m, 6H), 6.22 (s, 1H), 5.24−5.26 (d, J = 5.4 Hz, 1H), 4.00−4.19 (m, 3H), 3.73 (s, 6H), 3.08−3.10 (d, J = 5.7 Hz, 2H), 2.4 (s, 3H). ^{13}C NMR (300 MHz, $CDCl_3$-*d*): δ 162.2, 160.7, 158.5, 155.2, 153.9, 145.4, 136.2, 130.2, 128.2, 127.1, 126.9, 113.6, 113.0, 111.6, 101.7, 85.8, 70.6, 68.4, 64.6, 55.5, 18.6. HRMS-ESI (+) (m/z): $[M + H]^+$ calcd. for $C_{34}H_{33}O_7$, 553.2226; found: 553.2216.

1-(Bis(4-methoxyphenyl)(phenyl)methoxy)-3-((4-methyl-2-oxo-2*H*-chromen-7-yl)oxy)-propan-2-yl (2-cyanoethyl) diisopropylphosphoramidite (13). To a solution of compound **16** (226 mg, 0.50 mmol) in anhydrous CH_2Cl_2 (5 mL) under argon atmosphere, *N*,*N*-diisopropylethylamine (DIPEA) (156 μL, 0.9 mmol) was then added dropwise, followed by 2-cyanoethyl-*N*,*N*-diisopropylchlorophosphoramidite (167 μL, 0.75 mmol). The reaction mixture was stirred at room temperature for 3 h, then diluted by dichloromethane (30 mL), washed with $NaHCO_3$ (20 mL), and brine (20 mL), and dried over anhydrous sodium sulfate. The solvent was removed under reduced pressure. Upon purification by column chromatography (EtOAc:hexane:Et_3N = 40:59:1), the product **13** was isolated as a white foam (266 mg, 71%). ^{31}P NMR ($CDCl_3$-*d*, 300 MHz): δ 149.99, 149.67. ^1H NMR (DMSO-d_6): δ 7.12−7.43 (m, 10H), 6.71−6.80 (m, 6H), 6.06 (s, 1H), 4.02−4.26 (m, 3H), 3.42−3.75, 3.16−3.31 (m, 2H), 2.49−2.60 (m, 1H), 2.37−2.41 (m, 1H), 2.32 (s, 3H), 1.07−1.13 (m, 9H), 0.96−0.98 (d, J = 6.6 Hz, 3H). ^{13}C NMR (300 MHz, $CDCl_3$-*d*): δ 160.8, 160.2, 157.5, 154.2, 151.5, 143.6, 134.9, 129.1, 127.2, 126.8, 125.8, 124.6, 116.6, 112.7, 112.1, 111.5, 111.4, 111.0, 100.7, 85.2, 70.9, 70.7, 70.5, 70.3, 68.3, 68.1, 62.4, 57.5, 57.2, 54.2, 42.3, 42.1, 29.7, 23.4, 19.3, 19.1, 17.7. HRMS-ESI (+) (m/z): $[M + H]^+$ calcd. for $C_{43}H_{50}N_2O_8P$, 753.3305; found: 753.3295.

Synthesis of Coumarin-dT and Coumarin−Coumarin Dimers. A solution of 4-methyl-7-methoxy-2H-chromen-2-one (**1**, 38 mg, 0.2 mmol) and dT (146 mg, 0.6 mmol) in methanol (200 mL) was irritated with UV light at 350 nm for 3 days at room temperature. After removing solvent under reduced pressure, products were isolated upon purification by column chromatography.

7-(4-Hydroxy-5-(hydroxymethyl)tetrahydrofuran-2-yl)-3-methoxy-10*a*,10*b*-dimethyl-6*b*,7,10*a*,10*b*-tetrahydro-6*H*-chromeno[4′,3′:3,4]cyclobuta[1,2-*d*]pyrimidine-6,8,10-(6*aH*,9*H*)-trione (17). (CH_2Cl_2:MeOH = 95:5, a yellowish oil, 13 mg, 15%). ^1H NMR (300 MHz, DMSO-d_6): δ 7.18, 7.21 (d, J = 8.7 Hz, 1H), 6.70−6.73 (m, 1H), 6.51−6.53 (t, J = 2.4 Hz, 1H), 5.88 (m, 1H), 4.78, 4.82 (d, J = 9.3 Hz, 1H), 4.19−4.21 (t, J = 2.4 Hz, 1H), 4.04 (s, 3H), 3.64 (s, 2H), 3.28, 3.31 (d, J = 9.3 Hz, 1H), 1.99−2.06 (m, 2H), 1.56 (s, 3H), 1.27 (s, 3H). ^{13}C NMR (300 MHz, DMSO-d_6): δ 172.4, 164.7, 159.8, 151.5, 151.3, 128.7, 116.5, 111.2, 101.7, 87.3, 85.7, 83.3, 70.8, 62.0, 55.8, 52.3, 52.4, 46.9, 22.8, 22.6, 18.3, 17.9. HRMS-ESI (+) (m/z): $[M + H]^+$ calcd. for $C_{21}H_{25}N_2O_8$, 433.1605; found: 433.1612.

10-(4-Hydroxy-5-(hydroxymethyl)tetrahydrofuran-2-yl)-3-methoxy-6*b*,10*b*-dimethyl-8,10,10*a*,10*b*-tetrahydro-6*H*-chromeno[3′,4′:3,4]cyclobuta[1,2-*d*]pyrimidine-6,7,9-(6*aH*,6*bH*)-trione (18). (CH_2Cl_2:MeOH = 95:5, a yellowish oil, 8 mg, 9.2%). ^1H NMR (300 MHz, DMSO-d_6): δ 10.65 (s, 1H), 7.20, 7.23 (d, J = 8.7 Hz, 1H), 6.79−6.82 (m, 1H), 6.65, 6.66 (d, J = 2.4 Hz, 1H), 5.97−6.02 (m, 1H), 5.06, 5.08 (d, J = 3.6 Hz, 1H), 4.50 (s, 1H), 4.03−4.10 (m, 3H), 3.78 (s, 3H), 3.16−3.18 (m, 3H), 1.77 (m, 2H), 1.36 (s, 3H), 1.01 (s, 3H). ^{13}C NMR (300 MHz, DMSO-d_6): δ 172.5, 163.8, 160.0, 151.7, 130.9, 114.3, 111.2, 102.6, 87.3, 84.1, 71.7, 62.1, 55.9, 52.7, 52.2, 50.3, 49.1, 42.7, 42.0, 37.9, 27.1, 20.4. HRMS-ESI (+) (m/z): $[M + H]^+$ calcd. for $C_{21}H_{25}N_2O_8$, 433.1605; found: 433.1615.

3,9-Dimethoxy-6*b*,12*b*-dimethyl-12*a*,12*b*-dihydrocyclobuta-[1,2-*c*:3,4-*c*′]dichromene-6,12(6*aH*,6*bH*)-dione (19). (CH_2Cl_2:MeOH = 99:1, a white solid, 5.6 mg, 15%). ^1H NMR (300 MHz, $CDCl_3$-*d*): δ 6.97−7.04 (m, 2H), 6.70−6.73, 5.98−5.99 (m, 2H), 6.56−6.00 (m, 2H), 3.76, 3.60 (s, 6H), 3.35, 3.31 (s, 2H), 1.60, 1.18 (s, 6H). ^{13}C NMR (300 MHz, $CDCl_3$-*d*): δ 165.0, 163.7, 159.3, 150.7, 149.3, 127.0, 126.5, 114.0, 112.8, 111.0, 110.7, 101.4, 100.8, 54.6, 54.2, 45.6, 44.0, 40.0, 30.7, 25.4. HRMS-ESI (+) (m/z): $[M + H]^+$ calcd. for $C_{22}H_{21}O_6$, 381.1338; found: 381.1346.

■ ASSOCIATED CONTENT

Ⓢ Supporting Information

NMR and HRMS-ESI spectra for all new compounds, MALDI-TOF-MS spectra for functional ODNs, ICL formation or cleavage study via ^{32}P-labeling method or fluorescence assay, and related kinetic study. This material is available free of charge via the Internet at http://pubs.acs.org.

■ AUTHOR INFORMATION

Corresponding Author

*E-mail: pengx@uwm.edu.

Notes

The authors declare no competing financial interest.

■ ACKNOWLEDGMENTS

We are grateful for financial support from the UWM Research Growth Initiative (RGI101 × 234), the Greater Milwaukee Foundation (Shaw Scientist Award), and Wisconsin Applied Research Grant (ARG) Award. We thank UWM graduate school for providing distinguished graduate student fellowship for Huabing Sun. We also thank Hye Young Eom from the

undergraduate research program for preparation and property study of coumarin **1**.

REFERENCES

(1) Brulikova, L.; Hlavac, J.; Hradil, P. *Curr. Med. Chem.* **2012**, *19*, 364.
(2) Noll, D. M.; Mason, T. M.; Miller, P. S. *Chem. Rev.* **2006**, *106*, 277.
(3) Dronkert, M. L.; Kanaar, R. *Mutat. Res.* **2001**, *486*, 217.
(4) Peng, X.; Ghosh, A. K.; Van Houten, B.; Greenberg, M. M. *Biochemistry* **2010**, *49*, 11.
(5) Peng, X.; Pigli, Y. Z.; Rice, P. A.; Greenberg, M. M. *J. Am. Chem. Soc.* **2008**, *130*, 12890.
(6) Weng, M. W.; Zheng, Y.; Jasti, V. P.; Champeil, E.; Tomasz, M.; Wang, Y.; Basu, A. K.; Tang, M. S. *Nucleic Acids Res.* **2010**, *38*, 6976.
(7) Banerjee, A.; Santos, W. L.; Verdine, G. L. *Science* **2006**, *311*, 1153.
(8) Mishina, Y.; He, C. *J. Am. Chem. Soc.* **2003**, *125*, 8730.
(9) Duguid, E. M.; Mishina, Y.; He, C. *Chem. Biol.* **2003**, *10*, 827.
(10) Rusling, D. A.; Nandhakumar, I. S.; Brown, T.; Fox, K. R. *Chem. Commun.* **2012**, *48*, 9592.
(11) Zewail-Foote, M.; Hurley, L. H. *J. Am. Chem. Soc.* **2001**, *123*, 6485.
(12) Asai, A.; Nagamura, S.; Saito, H.; Takahashi, I.; Nakano, H. *Nucleic Acids Res.* **1994**, *22*, 88.
(13) Liu, Y.; Rokita, S. E. *Biochemistry* **2012**, *51*, 1020.
(14) Wang, H.; Wahi, M. S.; Rokita, S. E. *Angew. Chem., Int. Ed.* **2008**, *47*, 1291.
(15) Weinert, E. E.; Dondi, R.; Colloredo-Melz, S.; Frankenfield, K. N.; Mitchell, C. H.; Freccero, M.; Rokita, S. E. *J. Am. Chem. Soc.* **2006**, *128*, 11940.
(16) Zhou, Q.; Rokita, S. E. *Proc. Natl. Acad. Sci. U. S. A.* **2003**, *100*, 15452.
(17) Browne, W. R.; Feringa, B. L. *Annu. Rev. Phys. Chem.* **2009**, *60*, 407.
(18) Chung, J. W.; Lee, K.; Neikirk, C.; Nelson, C. M.; Priestley, R. D. *Small* **2012**, *8*, 1693.
(19) Majumdar, A.; Muniandy, P. A.; Liu, J.; Liu, J. L.; Liu, S. T.; Cuenoud, B.; Seidman, M. M. *J. Biol. Chem.* **2008**, *283*, 11244.
(20) Shahid, K. A.; Majumdar, A.; Alam, R.; Liu, S. T.; Kuan, J. Y.; Sui, X.; Cuenoud, B.; Glazer, P. M.; Miller, P. S.; Seidman, M. M. *Biochemistry* **2006**, *45*, 1970.
(21) Thazhathveetil, A. K.; Liu, S. T.; Indig, F. E.; Seidman, M. M. *Bioconjugate Chem.* **2007**, *18*, 431.
(22) Cimino, G. D.; Gamper, H. B.; Isaacs, S. T.; Hearst, J. E. *Annu. Rev. Biochem.* **1985**, *54*, 1151.
(23) Takasugi, M.; Guendouz, A.; Chassignol, M.; Decout, J. L.; Lhomme, J.; Thuong, N. T.; Helene, C. *Proc. Natl. Acad. Sci. U. S. A.* **1991**, *88*, 5602.
(24) Fujimoto, K.; Yamada, A.; Yoshimura, Y.; Tsukaguch, T.; Sakamoto, T. *J. Am. Chem. Soc.* **2013**, *135*, 16161.
(25) Yoshimura, Y.; Fujimoto, K. *Org. Lett.* **2008**, *10*, 3227.
(26) Li, H.; Broughton-Head, V. J.; Fox, K. R.; Brown, T. *Nucleosides, Nucleotides Nucleic Acids* **2007**, *26*, 1005.
(27) Li, H.; Broughton-Head, V. J.; Peng, G. M.; Powers, V. E. C.; Ovens, M. J.; Fox, K. R.; Brown, T. *Bioconjugate Chem.* **2006**, *17*, 1561.
(28) Trenor, S. R.; Shultz, A. R.; Love, B. J.; Long, T. E. *Chem. Rev.* **2004**, *104*, 3059.
(29) Musa, M. A.; Cooperwood, J. S.; Khan, M. O. *Curr. Med. Chem.* **2008**, *15*, 2664.
(30) Haque, M. M.; Sun, H.; Liu, S.; Wang, Y.; Peng, X. *Angew. Chem., Int. Ed.* **2014**, *53*, 7001−7005.
(31) Kool, E. T. *Chem. Rev.* **1997**, *97*, 1473.
(32) Sun, H.; Peng, X. *Bioconjugate Chem.* **2013**, *24*, 1226.
(33) Laing, B. M.; Barrow-Laing, L.; Harrington, M.; Long, E. C.; Bergstrom, D. E. *Bioconjugate Chem.* **2010**, *21*, 1537.
(34) Seidel, C. A. M.; Schulz, A.; Sauer, M. H. M. *J. Phys. Chem.* **1996**, *100*, 5541.
(35) Heinlein, T.; Knemeyer, J. P.; Piestert, O.; Sauer, M. *J. Phys. Chem. B* **2003**, *107*, 7957.
(36) Kendall, D. A.; MacDonald, R. C. *J. Biol. Chem.* **1982**, *257*, 13892.
(37) Zhang, B.-L.; Wang, F.-D.; Yue, J.-M. *Synth. Commun.* **2007**, *37*, 63.
(38) Chen, Y. L.; Lu, C. M.; Lee, S. J.; Kuo, D. H.; Chen, I. L.; Wang, T. C.; Tzen, C. C. *Bioorg. Med. Chem.* **2005**, *13*, 5710.

dx.doi.org/10.1021/jo5014756 | *J. Org. Chem.* XXXX, XXX, XXX−XXX